NCBI Bookshelf. A service of the National Library of Medicine, National Institutes of Health.

Nicolelis MAL, editor. Methods for Neural Ensemble Recordings. 2nd edition. Boca Raton (FL): CRC Press/Taylor & Francis; 2008.

Chapter 8 Defining Global Brain States Using Multielectrode Field Potential Recordings

Shih-Chieh Lin and Damien Gervasoni.

INTRODUCTION

Electrical activity is essential for neuronal communication. Over the years, in vivo multielectrode recordings have revealed that the electrical activities of individual neurons are not independent of each other. Instead, neurons tend to fire in a coordinated way within a given neural network. When measured as the electroencephalogram (EEG) or local field potential (LFP) signals, this neural coordination results in complex oscillatory activity patterns, which reflect synchronous synaptic potentials in a local network (Lopes da Silva 1991). Thus, unveiling the physiological mechanisms generating such complex oscillatory neural activity patterns is key to achieving a better understanding of how the brain operates in behaving animals.

The dynamics of the forebrain is not random. Ever since the initial discovery of cerebral electrical activity by Caton (Caton 1875) in rabbits and monkeys, and later in humans by Berger (Berger 1929), different patterns of forebrain activity have been tightly linked to various behavioral and wake-sleep states. Indeed, these distinct patterns of neural activity have become incorporated as part of the criteria of wake-sleep states (Green and Arduini 1954; Rechtschaffen and Kales 1968; Lopes da Silva and van Leeuwen 1969; Timo-Iaria et al. 1970; Moruzzi 1972; Winson 1972; Winson 1974; Gottesmann 1992; Steriade et al. 1993), suggesting that forebrain dynamics fall into several different regimes. This observation is intriguing because the same neural circuit can support several different dynamic regimes, which likely serve distinct roles in information processing and storage. Therefore, a quantitative description of its network dynamics can further reveal how the forebrain underlies so many fundamental functions in mammals.

In this chapter, we first describe the forebrain oscillatory activity patterns associated with different wake-sleep states, and highlight limitations of existing state identification methods. Then, we introduce a novel state-space framework (Gervasoni et al. 2004) that we have employed to quantitatively describe global forebrain dynamics in rodents. Such an analysis revealed several distinct regimes in which the forebrain can operate. These regimes correspond to distinct global brain states and are correlated with the occurrence of major wake-sleep states observed in both rats and mice. In addition, the state-space framework proposed here has allowed us to characterize the gradient dynamics within global brain states, providing a quantitative description of state transition dynamics in rodents. We end this chapter by discussing the underlying driving forces and potential functional roles of global brain states.

FOREBRAIN DYNAMICS IN DIFFERENT WAKE-SLEEP STATES

In mammals, the wake–sleep cycle consists of periodic alternation of three major behavioral states: waking (WK), slow-wave sleep (SWS), and rapid-eye-movement (REM) sleep. In conjunction with prominent changes in the behavior of the animal, these behavioral states are associated with remarkably different forebrain dynamics (Figure 8.1C). During WK, animals interact with their environment either actively or passively to acquire information about their immediate surrounding space. At the same time, cortical activity is dominated by low-amplitude fast oscillations (beta and gamma frequency bands, >20Hz) (Figure 8.1D) (Murthy and Fetz 1992; Steriade et al. 1993; Maloney et al. 1997; Rols et al. 2001). As the animal actively explores the environment, LFP activity displays prominent theta oscillations (5–7 Hz), especially in the hippocampus (Winson 1974; Buzsaki et al. 1990). These oscillations are modulated according to the level of arousal, attention, motor activity, and the presence or absence of incoming stimuli (Murthy and Fetz 1996; Fries et al. 2001; Fell et al. 2003; Buzsaki and Draguhn 2004).

In contrast to WK, sleep appears as a periodical state of quiescence, in which there is minimal processing of incoming sensory information. The behavioral hallmark of this state could thus be summarized as a suspension of the activities of the waking state. However, sleep is not defined by a homogenous state. At the very least, it can be divided into two distinct states, each named after its main neurophysiological features. As animals fall asleep, slow coherent

oscillations emerge in the cerebral cortex in different frequency bands (delta waves 1–4 Hz and spindles 7–14 Hz) (Steriade and McCarley 1990; Steriade et al. 1993) characterizing a first sleep state called slow-wave sleep, or non-REM sleep. These oscillations are organized into complex wave sequences by a very slow oscillation (usually 0.6–1 Hz) (Amzica and Steriade 1995; Contreras and Steriade 1995), and are concomitant with a progressive sensory disconnection (Moruzzi 1972; Steriade and McCarley 1990). As SWS deepens, spindling activities tend to decrease while delta waves become more prominent, with an intensity that correlates with the duration of the preceding awake state (Dijk et al. 1990).

After a certain time spent in SWS, a second sleep state ensues, characterized in humans by dreaming and conspicuous REM. Appropriately, this state has been named *REM sleep* (Aserinsky and Kleitman 1953; Dement and Kleitman 1957). During REM sleep, the cortical activity is quite similar to that observed during WK (Winson 1974; Borbely et al. 1984). That means that, for instance, in rats prominent gamma oscillations (Maloney et al. 1997; Gross and Gotman 1999) and theta oscillations (Vanderwolf 1969) are observed during this sleep state.

Although cortical activity of REM sleep is remarkably similar to that of WK, the functional sensory disconnection of the cortex reaches a maximum and motor output is actively suppressed (Dement and Kleitman 1957; Jouvet et al. 1959; Jouvet 1962). This has motivated some authors to propose an alternative nomenclature for REM sleep, calling it either *activated* (Aserinsky and Kleitman 1953) or *paradoxical sleep* (Jouvet 1962).

Limitations of Existing State Identification Algorithms

The various behavioral and neurophysiological features associated with wake-sleep states have led many to propose objective criteria to classify such states (Rechtschaffen and Kales 1968; Datta and Hobson 2000). Thus, the sleep research community has adopted polysomnographic criteria to identify wake-sleep states based on the activity patterns of EEG/LFP, electromyograms (EMGs), and electro-oculogram (EOG), in addition to behavioral criteria. EMG activity is maximal during WK, when the animal actively explores the environment and decreases as the animal enters SWS. During REM, the EMG activity is absent and the animal becomes atonic. EOG activity, on the other hand, is lowest during SWS and becomes prominent during REM. In rodents (Timo-Iaria et al. 1970; Datta and Hobson 2000), REM sleep is characterized by occasional whisker movements instead of eye movements, as well as particular sleep postures resulting from atonia. Although wake-sleep states have traditionally been coded by trained sleep researchers or clinicians based on polysomnographic criteria, many automatic state identification algorithms have been developed to provide objective and consistent coding of wake-sleep states, based on quantitative measures of EEG and EMG features (Robert et al. 1999).

Despite these efforts to identify wake-sleep states based on physiological features, most state-coding algorithms, both manual and automatic, face several important limitations. First, most algorithms implicitly assume that the wake–sleep cycle consists of several categorically different and predefined stable states. This approach tends to characterize the wake–sleep cycle as a stair case process, jumping back and forth between a set of states (Figure 8.1D, lower panel). Yet, this assumption is unlikely to be true when different stages of SWS (e.g., stage 1 through 4 non-REM sleep) appear as different as two categorically different states (e.g., WK versus SWS) in the stair case representation.

Second, the stair case representation of states further promotes the unrealistic view that state transitions occur instantaneously, with no intermediate periods between them, even when the dynamics of the system does not clearly resemble any predefined states.

Third, different state-coding algorithms have used different physiological measures and criteria to define states, making comparisons across algorithms difficult. To make matters worse, the number of states identified in different algorithms ranges from two to as many as eight (Kleinlogel 1990; Gottesmann 1992).

Fourth, because wake-sleep states result from broad changes in neuronal activity, ultimately, distinct internal brain states should be differentiated based on neuronal signals alone, without the need to rely on EMG signals. Yet, few algorithms have succeeded in that regard (Robert et al. 1996). These limitations and inconsistencies among algorithms signify the lack of a coherent framework to quantitatively describe the forebrain dynamics in different wake-sleep states.

STATE-SPACE FRAMEWORK REVEALS GLOBAL BRAIN STATES

Five years ago, we set out to develop a novel framework to quantitatively describe the type of global forebrain dynamics that defines distinct awake-sleep states. This novel approach was based primarily on analyzing the spectral information of LFPs. To avoid the limitations of the state-coding algorithms originating from predefining a set of categorically different states, we took the alternative approach. This involved representing the LFP spectral information with continuous-scale spectral features. Our assumption at the time was that if appropriate spectral features were chosen, one would be able to not only reveal global dynamic states generated by the forebrain, but also provide highly quantitative descriptions of the transition processes involved in switching from one state to another. Furthermore, because behavioral states are known to be associated with different forebrain dynamics, the spectral features we chose should also be able to separate the major behavioral states generated by our subjects (rats and mice). Such a framework could further address questions such as: how many distinct brain states really exist? Are these dynamic states different categorically or part of a continuous spectrum? Do state transitions follow stereotypical sequences?

In the next section we describe the approach that allowed us to implement the novel state-space framework required to address these broad issues (Gervasoni et al. 2004).

Data Collection

Initially, LFP signals were collected in adult rats through chronically implanted microelectrode arrays in several forebrain regions, including the primary somatosensory "barrel" cortex, hippocampus, dorsal striatum, and the ventral posterior medial nucleus of the thalamus (Gervasoni et al. 2004). Rats were habituated to the recording chamber prior to the recording sessions. Brain activity was then recorded continuously for up to 120 h. LFPs were preamplified (500X), filtered (0.3–400 Hz), and digitized at 500 Hz using a digital acquisition card (National Instrument, Austin) and a Multi-Neuron Acquisition Processor (Plexon Inc., Dallas). Behaviors were videotaped and synchronized with LFP recordings.

Wake-sleep states were coded by two trained experimenters on the basis of commonly adopted polysomnographic criteria (behaviors and associated LFP activity) (Timo-Iaria et al. 1970; Kleinlogel 1990; Gottesmann 1992; Maloney et al. 1997; Fanselow and Nicolelis 1999). This coding, referred to as *behavioral state coding*, was used later for comparison with results obtained from our novel state-space method. Five behavioral states were coded (Figure 8.1C):

Active exploration (AE): Animal engaged in exploratory behavior (locomotion, whisking, sniffing), with low-amplitude cortical LFP, and high theta (5–9 Hz) and gamma (30–55 Hz) power.

Quiet waking (QW): Animal immobile (standing or sitting quietly) or engaged in "automatic" stereotyped behaviors (eating, drinking, grooming), with low-amplitude cortical LFP and relatively high theta and gamma activity but less than during AE.

Whisker twitching (WT): Animal immobile and standing, with rhythmic whisker movements (twitching) at the same frequency of underlying cortical-thalamic oscillations (7–12 Hz) (Fanselow and Nicolelis 1999). WT is a physiological state that occurs with variable prevalence in rats, ranging from 0 to 9% over a 24 h recording period (Nicolelis et al. 1995; Fanselow and Nicolelis 1999; Wiest and Nicolelis 2003; Gervasoni et al. 2004).

Slow-wave sleep (SWS): Animal lying immobile with eyes closed and slow regular respiratory movements. SWS begins with sleep spindles (10–14 Hz) superimposed to delta waves (1–4 Hz). As SWS deepens, delta oscillations become predominant, although isolated spindles can still be observed.

Rapid-eye-movement (REM): Animal immobile and atonic except for intermittent whisker and ear twitches, with low cortical LFP amplitude and very high theta and gamma power. Epochs containing spindles associated with hippocampal theta rhythm (intermediate sleep) were at that point scored as part of REM episodes (Gottesmann 1973; Mandile et al. 1996).

2-D State Space

To reveal the stable neuronal dynamic regimes of forebrain networks, we focused on investigating the spectral content of forebrain LFP activity. LFPs were represented in the frequency domain as power spectrogram (Figure 8.1D), with the amplitude of each frequency bin calculated every second of the data record. Consistent with our understanding of spectral patterns in different wake-sleep states, the spectrogram showed more theta and gamma oscillation power during WK and REM, and more delta and spindle oscillations during SWS.

The grouping of frequency bins into frequency bands indicated that different frequency bins were not independent of each other. The implication is that if covarying frequency bins were appropriately combined, the spectrogram could be represented with much fewer variables, while still preserving most of the information. In the literature of statistical pattern recognition (Webb 2002), this is equivalent to a dimension reduction problem, i.e., representing a high-dimensional data set (in our case, many frequency bins) with only a few variables (spectral features).

One commonly used dimension reduction technique is principal component analysis (PCA), which searches for linear combinations of original variables in the high-dimensional data set, called principal components (PC), that explain the maximal amount of variability of the original data. Successive PCs contain orthogonal combinations of original variables, and are sorted by the amount of variability each PC explains. Thus, most of the information of the high-dimensional data set could be represented by the first few PCs that account for most of the variability. When PCA was applied to the spectrogram, the first two PCs (Figure 8.2A, left panel) typically explained 70–80% of the total variability of the LFP spectrogram.* The spectral combinations of the first two PCs were similar in shape when calculated from different forebrain LFPs.

A different dimension reduction strategy, such as linear discriminant analysis, relies on the knowledge of underlying categories and searches for features that best differentiate these classes. In our case, we were interested in finding spectral features that at least can separate the three major wake-sleep states. Assuming multidimensional normal distribution of spectral amplitudes within each class, the discriminant features correspond to the difference of the average spectrum between wake-sleep states. As illustrated in Figure 8.2A (right panel), the main spectral difference between SWS and WK states is in the slow frequency oscillations (<20 Hz), whereas the spectrums of WK and REM mainly differ in the delta (1–4 Hz) and theta (5–9 Hz) oscillations in opposite directions.

The spectral features obtained from these two different approaches were qualitatively similar (Figure 8.2A), indicating that these two features preserved most of the information about LFP spectrograms and at the same time could differentiate behavioral states. Based on these features, we developed a 2-D state-space framework to represent the LFP spectral information (Figure 8.2B). While focusing on the same frequency bands revealed by these spectral features, we chose to represent them in the form of spectral amplitude ratios: x-axis 0–4.5/0–9 Hz and y-axis 0–20/0–55 Hz. These ratios were designed such that the numerator frequency band was always contained in the denominator frequency band, so that the ratios were bounded in the [0, 1] range. These ratios provided the advantage of within-animal normalization that does not depend on the absolute amplitude of LFP signals, and were therefore easier to interpret and compare across animals. These two spectral features were calculated for each second of LFP data, plotted as a point in the 2-D state space. Contiguous points in the state space can be joined to form state trajectories, which provide temporal dynamic information on how spectral patterns evolve through time. Moreover, the speed of spectral evolution can be quantified as the spatial distance between temporally adjacent points on the same trajectory, or trajectory speed.

Global Brain States

Initially, the 2-D state space revealed at least three well-defined clusters in each animal (Figure 8.3). The presence of clusters indicated that the forebrain dynamics preferentially spent time in those dynamic patterns. These clusters correspond to stable dynamic regimes of the forebrain network, i.e., the main global brain states observed in mammals. The demonstration of clearly separated clusters indicates that the three global brain states are categorically different dynamic regimes. To further confirm this result, we calculated the average trajectory speed on each part of the state space (Figure 8.3C). Regions of the state space where spectral features changed slowly coincided with the three main clusters, whereas regions of fast spectral changes corresponded to transitional zones between major clustfers. This result confirmed that clusters represent stable forebrain dynamic regimes: when the forebrain dynamics

entered one of the three attractor states, the system was quite stable and moved little. On the other hand, points between clusters represent transitions between global brain states.

GLOBAL BRAIN STATES: THE NEURAL CORRELATES OF WAKE-SLEEP STATES

As these spectral features were also optimized to distinguish between the three major behavioral states, it is important to evaluate how global brain states correspond to behaviorally coded wake-sleep states. When behavioral states were color-coded onto the state space, the three main clusters grossly corresponded to the three major wake-sleep states (Figure 8.3A). The SWS cluster occupied the upper-right quadrant because the prominent slow oscillations (0–20 Hz) lead to a high value on the y-axis, and the prominent delta oscillations (1– 4 Hz) lead to a high value on the x-axis. Both REM and WK clusters had smaller values on the y-axis compared to the SWS cluster. REM cluster was located to the left of the WK cluster because the highly prominent theta oscillations (5–9 Hz) during REM lead to smaller values on the x-axis. Although a considerable degree of interanimal variability is to be expected when recording from outbred laboratory animals, we found remarkable similarity across the state space obtained for different animals.* In all animals we investigated, the relative positions of the three major clusters were highly conserved.

State-Coding Algorithm

For a quantitative comparison between the state-space framework and behavioral state coding, we developed an algorithm to convert the continuous-scale state-space representation into discrete global brain states focusing on the three main clusters (Figure 8.4). The spirit of this algorithm was to take advantage of the well-separated clusters and the temporal information inherent in the state space, as opposed to treating each time point as an independent sample. Because we have demonstrated that the three major clusters were stable attractor states in the state space, we considered all short trajectories (less than 20 s) leaving and reentering a given cluster boundary without touching the boundaries of other clusters as random fluctuations of the same cluster. The system was considered to be moving toward a different state only after the trajectory leaves the cluster boundary for an extended period of time. Thus, points outside the initial cluster boundaries could also be assigned to the major states, depending on their temporal continuity with adjacent clusters. Data points not coded as any of the major states (15–20%) were labeled *state transitions* (Figure 8.4).

Cluster boundaries could be determined in one of two ways: (1) when enough data points were available (preferentially at least 24 h continuous recording), cluster boundaries could be determined objectively by identifying nonoverlapping contours in the 2-D histogram around the main clusters (Figure 8.4, upper panel); (2) In smaller datasets, however, cluster boundaries have to be manually determined. However, with the incorporation of state trajectory information, the choice of the actual cluster boundaries mattered less to the final state identifications.

Our state identification algorithm purposefully left state trajectories between clusters not assigned to particular states, because those epochs represented state transitions during which the dynamics of the forebrain network does not resemble any of the global brain states. This ensured that the global brain states we identified are physiologically homogeneous. State transitions were studied with trajectory analyses and will be discussed later.

Comparison Against Behavioral State Coding

State coding by this algorithm agreed with human behavioral scoring more than 90% of the time (Figure 8.4, lower panel). The general improvement of automatic state classification after the exclusion of transition points underscores the fact that human-assisted coding imposes a discrete classification scheme on a dataset that is by nature continuous. Accurate automatic classification simply does not provide state identification around state transitions (white breaks in the algorithm-generated state coding) (Figure 8.4, middle panel), which are better understood by way of trajectory analysis. In contrast, human-assisted classification always assigns one of two successive states to each data point. Because these discrete state boundaries often fail to match the underlying sharp spectral boundaries, human-assisted classification likely introduces false-positives. Furthermore, agreement between expert observers usually falls between 80 and 90% (Robert et al. 1999). Thus, the automatic state identification provided by the robust cluster topography of 2-D state spaces constitutes a more conservative, objective, and accurate method for state detection

than that provided by human behavioral state coding.

Validation against EMG Activity in Mice

We have also applied the state-space framework to describe the forebrain dynamics of wild-type mice. Using LFPs recorded from mice hippocampus, similar clusters and topography were observed (Figure 8.5A and Figure 8.5B). As one distinctive feature of REM state is the lack of muscle tone, the REM epochs should have much lower EMG activity. As predicted, when neck muscle EMG activity was plotted as the third dimension of the state space, REM epochs showed little or absent EMG activity, while the adjacent WK cluster had maximal EMG activity (Figure 8.5C).

Taken together, these experiments demonstrated the existence of at least three global brain states in both rats and mice. We further showed a strong correspondence between global brain states and behaviorally coded wake-sleep states. These results indicate that global brain states represent the neural correlates of wake-sleep states.

GRADIENTS AND FUNCTIONAL SUBDIVISIONS WITHIN GLOBAL BRAIN STATES

In addition to the categorically different global brain states represented by the main clusters, several observations indicated that gradient subdivisions exist within the global brain states, especially within the SWS and WK clusters.

The SWS cluster was typically elongated with an elliptical shape. The two poles of the cluster were asymmetric because the SWS cluster connected with other clusters only through one pole. Further supporting this asymmetry, we observed that within the SWS clusters, there were graded changes in the average spectral power and coherence in multiple frequency bands over the long axis of the cluster (Figure 8.6). The pole of entrance and exit of the SWS cluster showed higher spindle power (8–14 Hz), whereas the other pole of SW showed more prominent delta activity (1–4 Hz). Parallel changes in spectral coherence were also observed. These graded differences within the SWS cluster resemble the distinction between light and deep SWS. As animals fall asleep, the light SWS is characterized by more spindle activity, whereas deep SWS is characterized by more delta oscillations. These observations also suggest that the distinction between light and deep SW is a graded one, but not a categorical one.

Similarly, asymmetry and gradients were observed in the WK cluster (Figure 8.6). The WK cluster was comprised of a main cluster with an extension on the left side toward the REM cluster. The WK cluster connected with other clusters primarily through the main cluster, but not through the leftward-extending part. Graded changes in theta oscillation (5–8 Hz) power and coherence were observed along the horizontal axis of the WK cluster, with theta oscillations being more prominent on the left side of the WK cluster.* A similar gradient was also observed for gamma oscillation (25–55 Hz) power. This division of the WK cluster corresponds to the behavioral distinction between QW and AE epochs, with the main WK cluster corresponds to QW epochs and the AE epochs correspond to the leftward extension of the WK cluster (see Figure 8.3A). This distinction also appears to be a graded subdivision and could reflect variations in the attentional and arousal levels within the WK state.

The state-space representation using continuous scales thus provides quantitative descriptions of gradient substates within global brain states. Such functional subdivision within the main behavioral states could contribute to, and potentially account for, variabilities observed at behavioral and neurophysiological levels. These observations also demonstrate that overlaying state-dependent information on the 2-D state space provides a comprehensive assessment of all behavioral states at the same time.

FOREBRAIN DYNAMICS DURING STATE TRANSITIONS

The 2-D state space also provides information about the temporal dynamics of state evolution in the form of "state trajectories." The trajectory information is most valuable when one intends to study how forebrain dynamics evolves from one state to another, defining a series of state transition processes. In the state space, state transitions can be defined as trajectories directly connecting two clusters. These state-transition trajectories turned out to have well-defined stereotypical trajectory patterns, along with characteristic transition durations (Figure 8.7A).

Several examples of state transitions are illustrated in Figure 8.7A. The first two state transition trajectories,

WK→SWS and REM→WK, represent typical fast state transitions with straight paths linking the two clusters. The durations of these trajectories are typically less than 20 s. Inspection of the corresponding LFP epochs showed that these state transitions were typically fast and steplike (Figure 8.7A, right panel in the top two rows), without involving an intermediate stage during the transition.* The other state transition in this category is SWS→WK (data not shown).

The most notable finding resulting from state trajectory analyses was the clear demonstration of the intermediate stage of sleep (IS) (Gottesmann 1996). Even though IS epochs were not behaviorally scored, IS state was clearly identified in three state transition trajectories: SWS→IS→REM, SWS→IS→WK and REM→IS→WK (Figure 8.7A, three lower rows). These state trajectories invariantly traversed through the left upper corner of the state space with stereotypical pathway patterns. Unlike the fast transitions with straight trajectories discussed in the last paragraph, these trajectories were curved and lasted longer than 30 s, indicating the presence of an intermediate stage during the transitions. The presence of an intermediate stage was further evidenced by the reduced trajectory speed in the left upper corner of the state space compared to areas around it (Figure 8.3C), indicating the presence of a relatively stable regime. The corresponding LFPs showed prominent oscillations present simultaneously in all forebrain regions (Figure 8.7A, right panel in the three lower rows).

The upper left corner of the state space where IS state is located corresponds to LFP epochs with high-amplitude low-frequency (<20 Hz) oscillations (y-axis) and high-amplitude theta oscillations (x-axis) (Figure 8.6). These properties are consistent with the description of IS, characterized by high-amplitude spindle oscillations in the cortex and prominent theta oscillations in the hippocampus (Gottesmann 1996). Our observation that high-amplitude spindle oscillations were present in all forebrain regions led to the demonstration that these oscillations were coherent across forebrain regions over a wide frequency range (8–20 Hz) (Figure 8.7B). Indeed, the IS state possessed the highest coherence in this frequency range in the entire state space (Figure 8.6).

These results also reveal that when animals wake up from SWS, two possible and parallel transition sequences exist, through SWS→WK or through SWS→IS→WK. Although the two transitions could be behaviorally indistinguishable, they could have opposite effects on the learning ability in rats (Vescia et al. 1996). Our results therefore strongly argue that the IS state should be independently identified in any state-coding algorithms designed to describe the structure of sleep.

GENERAL DISCUSSION

Advantages and Limitations of the State-Space Framework

We described a novel yet simple and quantitative state-space framework to describe the dynamics of the forebrain network. The 2-D state space not only reveals categorically different global brain states, but also depicts gradient substates. Furthermore, it provides quantitative descriptions of state transition processes.

The success of state-space framework relies on the proper choice of two continuous-scale spectral amplitude ratios. Using PCA to extract spectral features has been previously attempted with good success (Jobert et al. 1994; Makeig and Jung 1995; Corsi-Cabrera et al. 2001). The state-space framework further demonstrated that combining two spectral features provided unequivocal state identification that could not be achieved using either feature alone. Although the spectral features we choose successfully identified the main global brain states, we do not claim that these spectral features are optimal. Spectral features that focused on similar frequency bands, such as the ones shown in Figure 8.2A, provided similar cluster separation (data not shown). However, the use of continuous-scale spectral features in a 2-D space should be widely adopted in future descriptions of global brain states.

The problem of feature extraction and dimension reduction is very difficult, especially when the target categories for classification remain unknown. It remains possible that other dimension reduction techniques might provide useful spectral features and identify more dynamics states. Especially, future methods could improve upon the poor temporal resolution in the state-space method because of the smoothing procedure. However, given the relatively slow temporal evolution of behavioral states, such slow temporal dynamics are likely well captured by the state-space framework.

We further demonstrated a tight coupling between global brain states and behaviorally coded wake-sleep states in both

rats and mice. It is important to recognize the distinction between global brain states, which is a description of forebrain dynamics, and behavioral states, which mainly considers the behavioral manifestations. Therefore, at least under normal physiological conditions, global brain states can be regarded as the neural correlates of behavioral states and could be used interchangeably. Whether they can be dissociated under extreme conditions or around state transition remains to be investigated. It also remains to be determined whether similar global brain states can be identified using EEG signals, and whether similar states exist in primates.

Unlike most state-identification algorithms (Robert et al. 1999), the state-space framework relies only on neural signals, and does not require EMG activity or access to overt behaviors of the animal. More importantly, it can correctly depict all wake-sleep states without any human supervision. Therefore, the automatic state coding algorithm outlined here, by excluding state transition epochs, provides state identifications that are physiologically more homogeneous than behavioral state coding. Finally, the identification of the IS state with distinct physiological properties and unique roles in several state transition sequences strongly suggests that IS state should be routinely coded as a separate physiological entity (Gottesmann 1996).

In summary, the state space provides a unifying framework to describe the dynamics of forebrain network throughout the whole wake–sleep cycle. The global brain states revealed here represent the neural correlates of behavioral states.

The Driving Forces: Neuromodulatory Systems

The identification of global brain states relies only on LFP spectral patterns, which reflect the summation of synaptic potentials and intrinsic currents, the amplitude of which is correlated to the degree of coherent activity in a population of neurons. These coherent activities are generated either locally or through long-range interactions between different forebrain regions.

The existence of multiple dynamic regimes in the same anatomical forebrain network is intriguing. Previous work in invertebrate systems has demonstrated that anatomical connectivity alone does not determine the dynamics of the system (Marder 1998; Selverston et al. 1998). Even in simple networks of 30 neurons where the circuit connectivity has been completely mapped out, these networks are capable of generating different dynamic patterns that cannot be derived directly from the connectivity. Instead, the dynamics of the network is mainly determined by short-term synaptic plasticity and, most importantly, by neuromodulatory inputs.

The same design principle is probably preserved evolutionarily as an efficient mechanism to dynamically modulate the activity of the mammalian forebrain. Global brain states are associated with, and directly modulated by, systematic changes in neuromodulatory activity arising from ascending neuromodulatory systems, including the pontine and basal forebrain cholinergic nuclei (Gu 2002; Jones 2003). Based on microdialysis and recording of neuronal activity (Jones 2003), most neuromodulatory systems, including acetylcholine (ACh), norepinephrine (NE), serotonin (5-HT), and histamine (Hist) systems have been shown to be active during WK and decrease their activity during SWS. During REM sleep, however, monoaminergic systems (NE, 5-HT, and HIst) virtually shut down, and only the cholinergic system remains active (Figure 8.8). These neuromodulatory systems project extensively to the entire forebrain and exert great influences on the excitability of neurons and the amplitude of synaptic potentials through metabotropic receptors (Kaczmarek and Levitan 1987; Marder and Calabrese 1996), thus sculpturing the dynamics of the forebrain network in different ways across distinct behavioral states.

In conclusion, neuromodulatory systems serve as the main driving force that determines the dynamics of the forebrain network, which, in turn, gates neuronal responses and behavioral outputs (Figure 8.8). In that regard, global brain states can also be considered as neural correlates of the activity of the underlying neuromodulatory systems.

State-Dependent Information Processing and Memory Formation

At different behavioral states, the different global dynamic regimes, along with the neuromodulatory influences, impart different information processing capacities to the forebrain network. For instance, studies in awake monkeys performing a visual search task have shown that responses to visual stimulation recorded in area V4 were often reduced, or even completely blocked, when animals became drowsy, while the background activity changed to the

burst–pause pattern typically observed in sleep (Pigarev et al. 1997). Similarly, state-dependent alterations of auditory receptive fields have been reported in rats (Edeline et al. 2000; Edeline et al. 2001). In the somatosensory system, responses to tactile stimulations differ greatly during different behavioral states (Fanselow and Nicolelis 1999) and depend on whether the animal is actively or passively exploring its surrounding environment (Krupa et al. 2004). These results indicate that information processing is substantially altered by both internal dynamic brain states and the overall behavioral state of the animal. An accurate identification of brain states, such as the one provided by the state-space framework described here, defines a powerful tool for most neurophysiological experiments carried out in behaving animals.

Different regimes of information processing during different behavioral states further support different roles for the forebrain circuitry during learning and memory consolidation. Whereas wakefulness can be described as a state for real-time processing of sensory-motor information, several authors have proposed that sleep may be involved in the offline processing and consolidation of newly acquired information (Fishbein 1971; Hennevin et al. 1971; Smith 1985; Maquet 2001; Stickgold et al. 2001; Walker and Stickgold 2006). A wide range of animal studies have supported that REM sleep plays a critical role in procedural learning (Smith 1985, 1995). Smith proposed the existence of "REM windows" for memory consolidation, based on the observations that the amount of REM sleep increased in a particular time window after procedural training, and deprivation of REM sleep during this window leads to diminished retention (Smith 1985). Similarly, in human subjects, procedural learning such as visual texture discrimination (Karni et al. 1994) and motor sequence learning (Walker et al. 2002) significantly benefit from a night of sleep, but not from equivalent periods of waking.

CONCLUSIONS

Global brain states revealed by the state-space framework proposed here represent the neural correlates of behavioral wake-sleep states. These states can also be regarded as reflecting the underlying neuromodulatory drive provided by a vast and distributed neural circuitry (Figure 8.8). In addition to revealing the global brain states, the 2-D state space provides a quantitative description of gradient substates and state transition dynamics. As such, the 2-D state-space approach defines a novel and powerful method of studying state-dependent processes in behaving animals.

REFERENCES

1. Amzica F, Steriade M. Short- and long-range neuronal synchronization of the slow (< 1 Hz) cortical oscillation. J Neurophysiol. 1995;73(1):20–38. [PubMed: 7714565]
2. Aserinsky E, Kleitman N. Regularly occuring periods of ocular motility and concomitant phenomena during sleep. Science. 1953;118:361–375.
3. Berger H. Uber das Elektroenkephalogramm des menschen. Arch Psychiatr. 1929;87:527–570.
4. Borbely AA, Tobler I, et al. Effect of sleep deprivation on sleep and EEG power spectra in the rat. Behav Brain Res. 1984;14(3):171–82. [PubMed: 6525241]
5. Buzsaki G, Chen LS, et al. Spatial organization of physiological activity in the hippocampal region: relevance to memory formation. Prog Brain Res. 1990;83:257–68. [PubMed: 2203100]
6. Buzsaki G, Draguhn A. Neuronal oscillations in cortical networks. Science. 2004;304(5679):1926–1929. [PubMed: 15218136]
7. Caton R. The electric currents of the brain. Br Med J. 1875;2(1):278.
8. Contreras D, Steriade M. Cellular basis of EEG slow rhythms: a study of dynamic corticothalamic relationships. J Neurosci. 1995;15(1 Pt 2):604–22. [PubMed: 7823167]
9. Corsi-Cabrera M, Perez-Garci E, et al. EEG bands during wakefulness, slow-wave, and paradoxical sleep as a result of principal component analysis in the rat. Sleep. 2001;24(4):374–80. [PubMed: 11403521]
10. Datta S, Hobson JA. The rat as an experimental model for sleep neurophysiology. Behav Neurosci. 2000;114(6):1239–44. [PubMed: 11142656]
11. Dement WC, Kleitman N. Cyclic variations in EEG during sleep and their relation to eye movements, body motility and dreaming. Electroencephalogr Clin Neurophysiol. 1957;20:673–690. [PubMed: 13480240]
12. Dijk DJ, Brunner DP, et al. Electroencephalogram power density and slow wave sleep as a function of prior

waking and circadian phase. Sleep. 1990;13(5):430–40. [PubMed: 2287855]
13. Edeline JM, Dutrieux G, et al. Diversity of receptive field changes in auditory cortex during natural sleep. Eur J Neurosci. 2001;14(11):1865–80. [PubMed: 11860482]
14. Edeline JM, Manunta Y, et al. Auditory thalamus neurons during sleep: changes in frequency selectivity, threshold, and receptive field size. J Neurophysiol. 2000;84(2):934–52. [PubMed: 10938318]
15. Fanselow EE, Nicolelis MA. Behavioral modulation of tactile responses in the rat somatosensory system. J Neurosci. 1999;19(17):7603–16. [PubMed: 10460266]
16. Fell J, Fernandez G, et al. Is synchronized neuronal gamma activity relevant for selective attention? Brain Res Rev. 2003;42(3):265–272. [PubMed: 12791444]
17. Fishbein W. Disruptive effects of rapid eye movement sleep deprivation on long-term memory. Physiol Behav. 1971;6(4):279–82. [PubMed: 4337286]
18. Fries P, Reynolds JH, et al. Modulation of oscillatory neuronal synchronization by selective visual attention. Science. 2001;291(5508):1560–1563. [PubMed: 11222864]
19. Gervasoni D, Lin SC, et al. Global forebrain dynamics predict rat behavioral states and their transitions. J Neurosci. 2004;24(49):11137–47. [PubMed: 15590930]
20. Gottesmann C. [Intermediate stages of sleep in the rat] Rev Electroencephalogr Neurophysiol Clin. 1973;3(1):65–8. [PubMed: 4807416]
21. Gottesmann C. Detection of seven sleep-waking stages in the rat. Neurosci Biobehav Rev. 1992;16(1):31–8. [PubMed: 1553104]
22. Gottesmann C. The transition from slow-wave sleep to paradoxical sleep: evolving facts and concepts of the neurophysiological processes underlying the intermediate stage of sleep. Neurosci Biobehav Rev. 1996;20(3):367–87. [PubMed: 8880730]
23. Green JD, Arduini AA. Hippocampal electrical activity in arousal. J Neurophysiol. 1954;17:533–57. [PubMed: 13212425]
24. Gross DW, Gotman J. Correlation of high-frequency oscillations with the sleep-wake cycle and cognitive activity in humans. Neuroscience. 1999;94(4):1005–18. [PubMed: 10625043]
25. Gu Q. Neuromodulatory transmitter systems in the cortex and their role in cortical plasticity. Neuroscience. 2002;111(4):815–835. [PubMed: 12031406]
26. Hennevin E, Leconte P, et al. [Effect of acquisition level on the increase of paradoxical sleep duration due to an avoidance conditioning in the rat] C R Acad Sci Hebd Seances Acad Sci D. 1971;273(25):2595–8. [PubMed: 4334535]
27. Jobert M, Escola H, et al. Automatic analysis of sleep using two parameters based on principal component analysis of electroencephalography spectral data. Biol Cybern. 1994;71(3):197–207. [PubMed: 7918799]
28. Jones BE. Arousal systems. Front Biosci. 2003;8:s438–51. [PubMed: 12700104]
29. Jouvet M. [Research on the neural structures and responsible mechanisms in different phases of physiological sleep] Arch Ital Biol. 1962;100:125–206. [PubMed: 14452612]
30. Jouvet M, Michel F, et al. [On a stage of rapid cerebral electrical activity in the course of physiological sleep] C R Seances Soc Biol Fil. 1959;153:1024–8. [PubMed: 14408003]
31. Kaczmarek LK, Levitan IB. Neuromodulation: The biochemical control of neuronal excitability. New York: Oxford Univ. Press; 1987.
32. Karni A, Tanne D, et al. Dependence on REM sleep of overnight improvement of a perceptual skill. Science. 1994;265(5172):679–82. [PubMed: 8036518]
33. Kleinlogel H. Analysis of the vigilance stages in the rat by fast Fourier transformation. Neuropsychobiology. 1990;23(4):197–204. [PubMed: 2130289]
34. Krupa DJ, Wiest MC, et al. Layer-specific somatosensory cortical activation during active tactile discrimination. Science. 2004;304(5679):1989–92. [PubMed: 15218154]
35. Lopes da Silva F. Neural mechanisms underlying brain waves: from neural membranes to networks. Electroencephalogr Clin Neurophysiol. 1991;79(2):81–93. [PubMed: 1713832]
36. Lopes da Silva F, van Leeuwen WS. Electrophysiological correlates of behaviour. Psychiatr Neurol Neurochir. 1969;72(3):285–311. [PubMed: 4899715]

37. Makeig S, Jung TP. Changes in alertness are a principal component of variance in the EEG spectrum. Neuroreport. 1995;7(1):213–6. [PubMed: 8742454]
38. Maloney KJ, Cape EG, et al. High-frequency gamma electroencephalogram activity in association with sleep-wake states and spontaneous behaviors in the rat. Neuroscience. 1997;76(2):541–55. [PubMed: 9015337]
39. Mandile P, Vescia S, et al. Characterization of transition sleep episodes in baseline EEG recordings of adult rats. Physiol Behav. 1996;60(6):1435–9. [PubMed: 8946487]
40. Maquet P. The role of sleep in learning and memory. Science. 2001;294(5544):1048–52. [PubMed: 11691982]
41. Marder E. From biophysics to models of network function. Annu Rev Neurosci. 1998;21(1):25–45. [PubMed: 9530490]
42. Marder E, Calabrese RL. Principles of rhythmic motor pattern generation. Physiol Rev. 1996;76(3):687–717. [PubMed: 8757786]
43. Moruzzi G. The sleep-waking cycle. Ergeb Physiol. 1972;64:1–165. [PubMed: 4340664]
44. Murthy VN, Fetz EE. Coherent 25- to 35-Hz oscillations in the sensorimotor cortex of awake behaving monkeys. Proc Natl Acad Sci U S A. 1992;89(12):5670–4. [PMC free article: PMC49354] [PubMed: 1608977]
45. Murthy VN, Fetz EE. Oscillatory activity in sensorimotor cortex of awake monkeys: synchronization of local field potentials and relation to behavior. J Neurophysiol. 1996;76(6):3949–67. [PubMed: 8985892]
46. Nicolelis MA, Baccala LA, et al. Sensorimotor encoding by synchronous neural ensemble activity at multiple levels of the somatosensory system. Science. 1995;268(5215):1353–8. [PubMed: 7761855]
47. Pigarev IN, Nothdurft HC, et al. Evidence for asynchronous development of sleep in cortical areas. Neuroreport. 1997;8(11):2557–60. [PubMed: 9261826]
48. Rechtschaffen A, Kales A. A manual of standardized terminology, techniques and scoring system for sleep stages of human subjects. U.S. Department of Health, Education and Welfare; Washington, D.C: 1968. [PubMed: 11422885]
49. Robert C, Guilpin C, et al. Automated sleep staging systems in rats. J Neurosci Methods. 1999;88(2):111–22. [PubMed: 10389657]
50. Robert C, Karasinski P, et al. Adult rat vigilance states discrimination by artificial neural networks using a single EEG channel. Physiol Behav. 1996;59(6):1051–60. [PubMed: 8737892]
51. Rols G, Tallon-Baudry C, et al. Cortical mapping of gamma oscillations in areas V1 and V4 of the macaque monkey. Vis Neurosci. 2001;18(4):527–40. [PubMed: 11829299]
52. Selverston A, Elson R, et al. Basic Principles for Generating Motor Output in the Stomatogastric Ganglion. Ann NY Acad Sci. 1998;860(1):35–50. [PubMed: 9928300]
53. Smith C. Sleep states and learning: a review of the animal literature. Neurosci Biobehav Rev. 1985;9(2):157–68. [PubMed: 3892377]
54. Smith C. Sleep states and memory processes. Behav Brain Res. 1995;69(1–2):137–45. [PubMed: 7546305]
55. Steriade M, McCarley RW. Brainstem control of wakefulness and sleep. New York: Plenum Press; 1990.
56. Steriade M, McCormick DA, et al. Thalamocortical oscillations in the sleeping and aroused brain. Science. 1993;262(5134):679–85. [PubMed: 8235588]
57. Stickgold R, Hobson JA, et al. Sleep, learning, and dreams: off-line memory reprocessing. Science. 2001;294(5544):1052–7. [PubMed: 11691983]
58. Timo-Iaria C, Negrao N, et al. Phases and states of sleep in the rat. Physiol Behav. 1970;5(9):1057–62. [PubMed: 5522520]
59. Vanderwolf CH. Hippocampal electrical activity and voluntary movement in the rat. Electroencephalogr Clin Neurophysiol. 1969;26(4):407–18. [PubMed: 4183562]
60. Vescia S, Mandile P, et al. Baseline transition sleep and associated sleep episodes are related to the learning ability of rats. Physiol Behav. 1996;60(6):1513–25. [PubMed: 8946500]
61. Wagner U, Gais S, et al. Sleep inspires insight. Nature. 2004;427(6972):352–355. [PubMed: 14737168]
62. Walker MP, Brakefield T, et al. Practice with sleep makes perfect: sleep-dependent motor skill learning. Neuron. 2002;35(1):205–11. [PubMed: 12123620]
63. Walker MP, Stickgold R. Sleep, memory, and plasticity. Annu Rev Psychol. 2006;57:139–66. [PubMed: 16318592]

64. Webb AR. Statistical Pattern Recognition. Wiley; 2002.
65. Wiest MC, Nicolelis MA. Behavioral detection of tactile stimuli during 7–12 Hz cortical oscillations in awake rats. Nat Neurosci. 2003 [PubMed: 12897789]
66. Winson J. Interspecies differences in the occurrence of theta. Behav Biol. 1972;7(4):479–87. [PubMed: 4340452]
67. Winson J. Patterns of hippocampal theta rhythm in the freely moving rat. Electroencephalogr Clin Neurophysiol. 1974;36(3):291–301. [PubMed: 4130608]

Footnotes

* LFP amplitude spectrograms were calculated by running a sliding window Fourier transform with window size 2 s and step size 1 s. The resulting spectrogram was further smoothed, per frequency bin, with a 10-bin Hanning window to reduce spectral variations and increase the reliability of PCA transformation. When smoothing was not used, the first two PCs explained about 40% variability.

* The only exception was the location of the WT cluster. The general spectra of WT were very similar across animals, with the dominant oscillation at 7–12 Hz and resonant frequencies at 14–18 and 20–28 Hz. However, the relative amplitude at the resonant frequencies was substantially different among animals. There is a positive correlation between the amount of WT in each animal and the relative power at the resonant frequencies. This spectral difference at the resonant frequencies among animals accounted for the varying location of the WT cluster in the 2-D state map.

* Notice that while the SWS cluster possessed more spectral power in the theta range compared to the REM and WK clusters, theta coherence was more prominent in the REM cluster and the left half of the WK cluster than that of the SWS cluster.

* As a result of temporal smoothing in constructing the state space, the duration of trajectories (<20 s) is visibly longer than the duration of state transition revealed by inspecting LFP traces. In these direct and fast state transitions, the duration of state transition trajectories therefore primarily reflected the length of smoothing kernel.

Figures

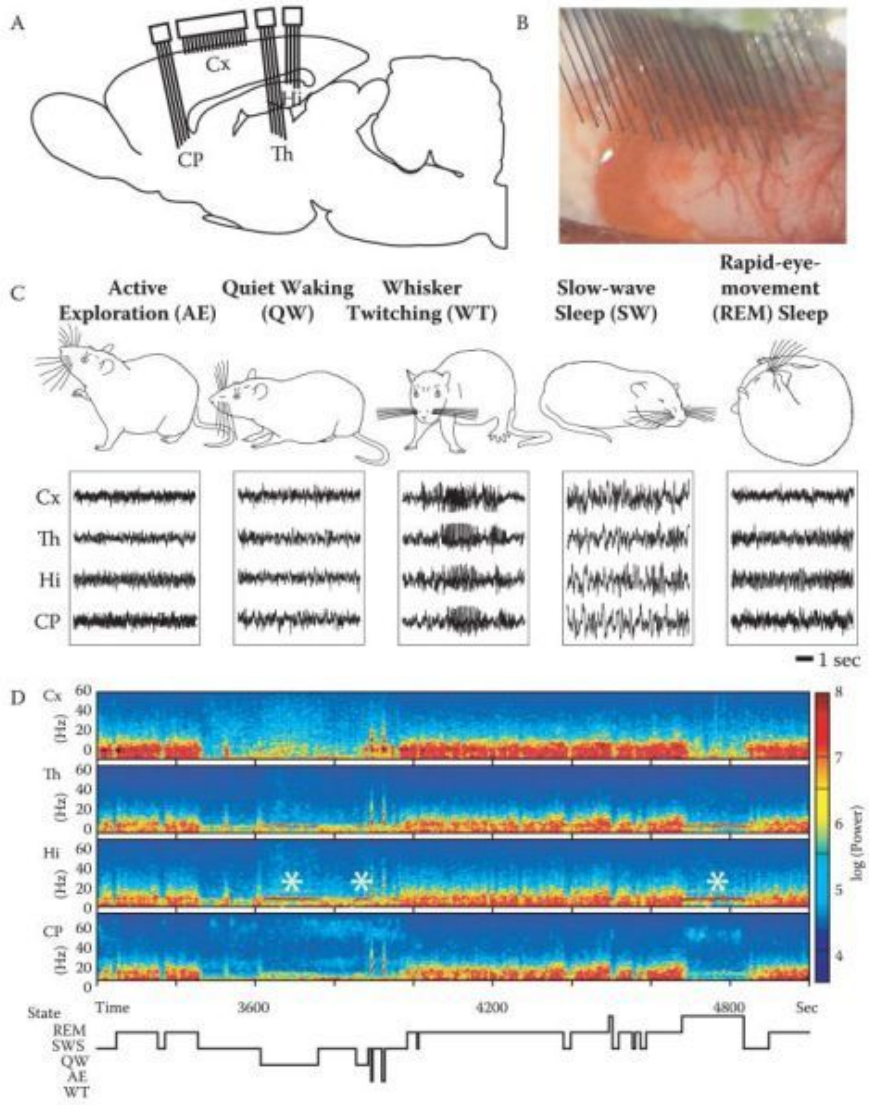

FIGURE 8.1

Local field potentials and behavioral states. (A) Schematic representation of the location of the multielectrode implants on a parasagittal section of a rat brain. The primary somatosensory cortex (Cx), the hippocampus (Hi), the ventromedial posterior nucleus of the thalamus (Th), and the caudate-putamen (CP) were implanted with microelectrode arrays. (B) Photograph of a 4 × 16 tungsten microwires array used for recordings in the somatosensory cortex (barrel field). (C) Raw simultaneous LFP recordings in the four fore-brain regions. Five behavioral states were coded based on behaviors and visual inspection of LFP traces. (D) LFP power spectrograms, aligned with staircase representation of behavioral states. All areas show simultaneous state-dependent variations of LFP spectral pattern. Note that AE and REM both show pronounced theta rhythm (white asterisk).

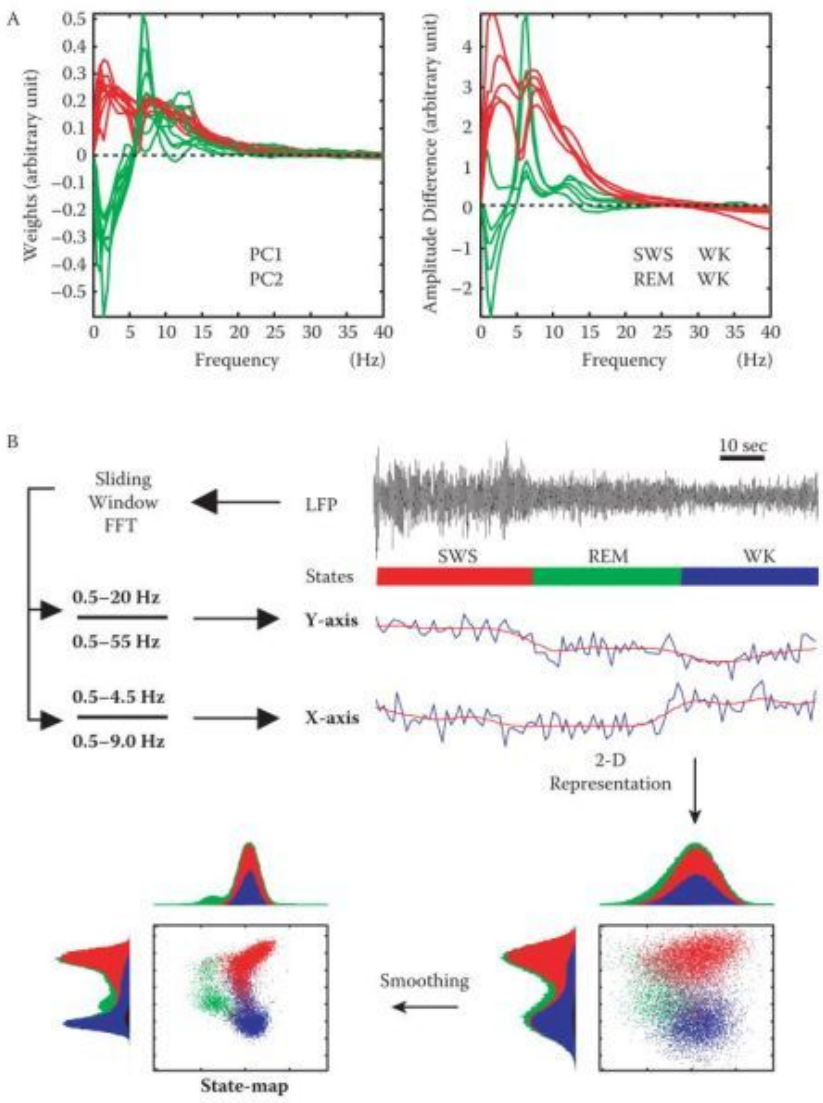

FIGURE 8.2

(See color insert following page 140.) Construction of state-space map. (A) Left panel, spectral features (PC1 and PC2) obtained by applying PCA to the spectrogram of individual forebrain LFPs in one rat. Right panel, difference of the average amplitude spectrum in different behavioral states. Each trace represents the result calculated from one forebrain LFP. Notice both methods obtained similar spectral features. (B) Construction of state-space map: A sliding window Fourier transform was applied to each LFP signal to calculate two spectral amplitude ratios at 1-sec temporal resolution. The spectral ratios obtained from individual LFPs were combined using PCA and represented by the first PC. The two PCs (blue traces) were further smoothed with a 20-bin Hanning window (red traces). The two smoothed spectral ratios define the 2-D state-space. Note that clear cluster structures emerged in the 2-D state-space after smoothing and that either feature along (1-D histogram) was insufficient for clear cluster separation. (Gervasoni, D. and Lin, S.C. et al. (2004). Global forebrain dynamics predict rat behavioral states and their transitions. *J Neurosci* 24(49): 11137–47.)

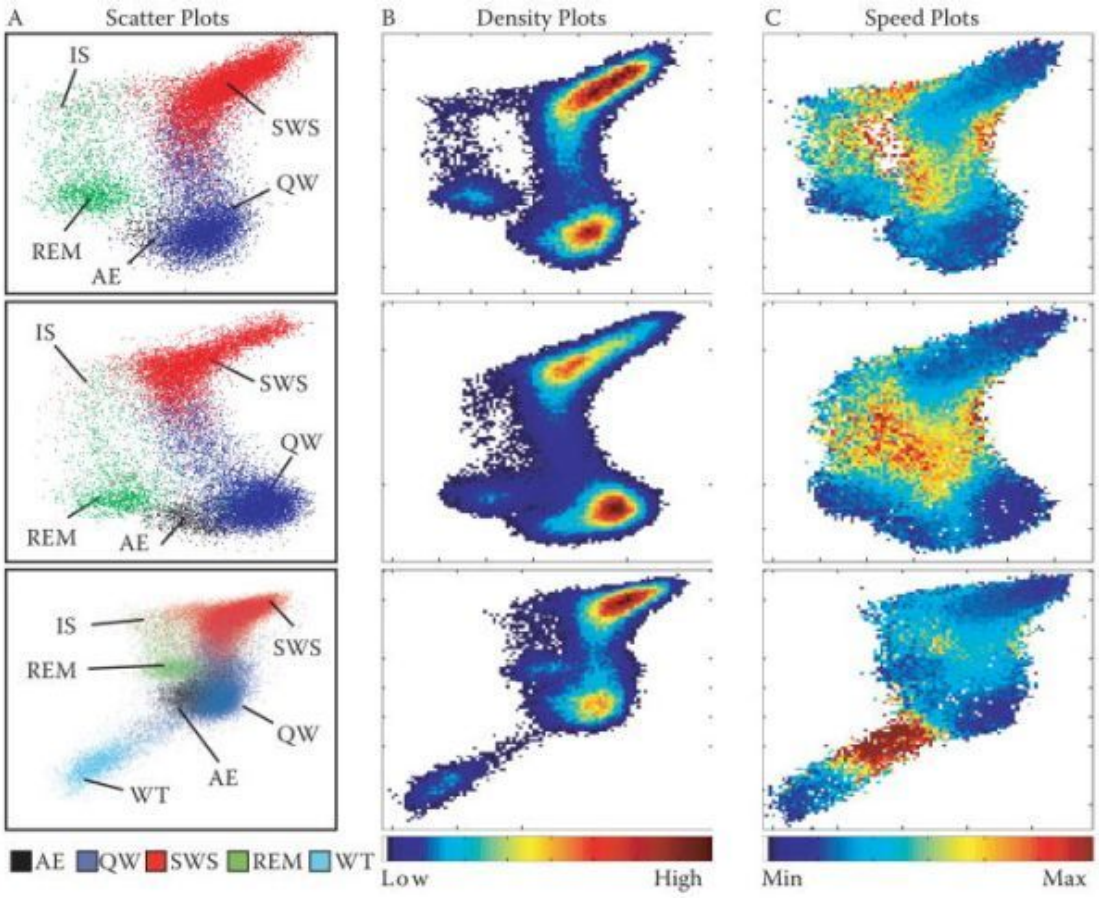

FIGURE 8.3

(See color insert following page 140.) Global brain states. (A) Scatter plots of the 2-D state space, color-coded for behaviorally coded states. Each dot corresponds to a 1 s window from which the amplitude ratios were calculated. For all animals, 48 h of recording is displayed; to avoid graphic saturation, only 20% of the data points were evenly sampled and plotted. Note that clusters correspond to behavioral states. (B) Density plots, calculated from the scatter plots, show the conserved cluster topography and the relative abundance of various states. (C) Speed plots representing the average velocity of spontaneous trajectories within the 2-D state-space. Stationarity (low speed) can be observed within the three main clusters, whereas the maximum speed is reached during transitions from one cluster to another, i.e., between brain states. IS, intermediate sleep. (Gervasoni, D. and Lin, S.C. et al. (2004). Global forebrain dynamics predict rat behavioral states and their transitions. *J Neurosci* 24(49): 11137–47.)

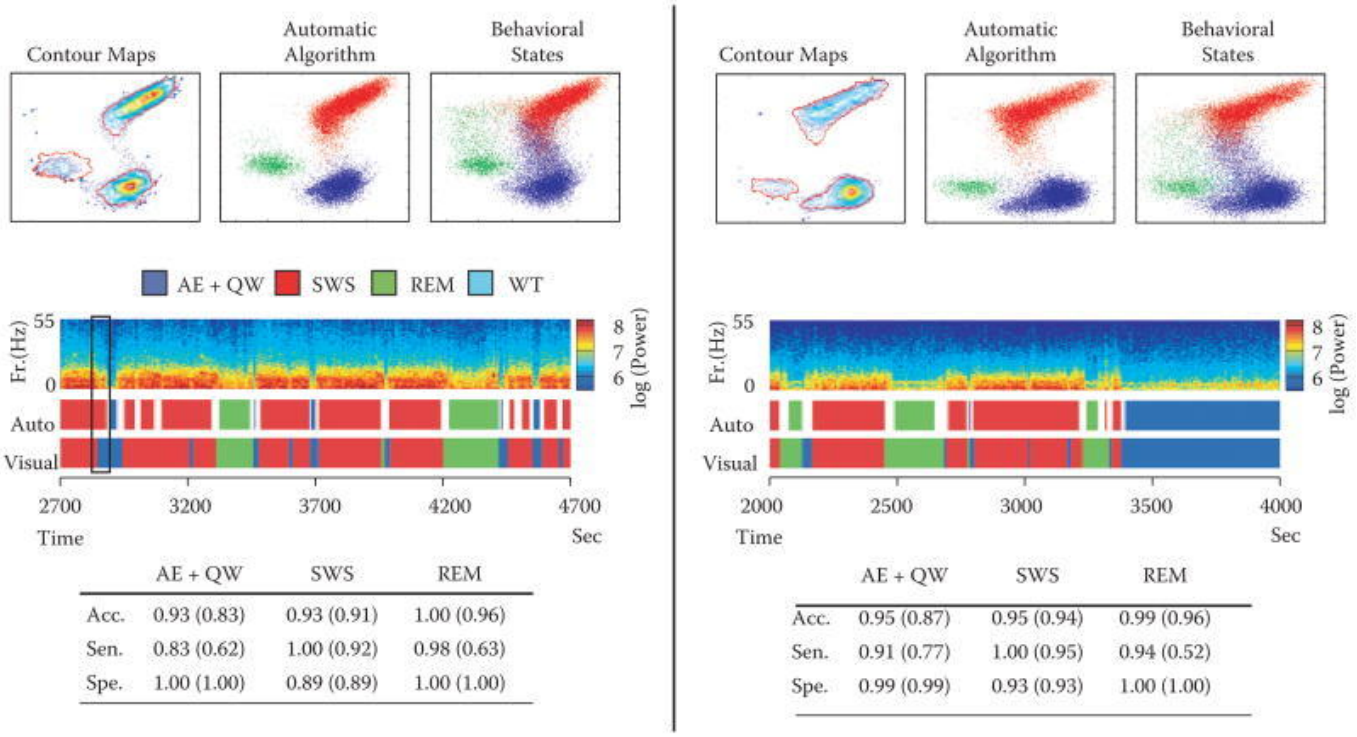

FIGURE 8.4

Automatic state-coding algorithm. Comparison of automatic state-coding with behavioral states in two rats. Upper panel, contour maps show cluster boundaries (red contour) corresponding to the three main clusters. State labels were color-coded and overlaid on the scatter plot for the automatic algorithm (middle panel) and the behaviorally coded states (right panel). Note that trajectories transiently wandered off cluster boundaries were still identified by the automatic algorithm as the three main states. The automatic algorithm provides a conservative, but physiologically more homogeneous, state assignment compared to behavioral state coding. Middle panel, an example LFP spectrogram (2000 s segment) aligned with color-coded states obtained by the automatic algorithm and behavioral coding. Automatic and behavioral-coded classifications show a very high degree of agreement, but differ occasionally around state transitions. (inset in spectrogram). Lower panel, quantitative comparisons of the two state classification methods. The parameters compared were: (i) accuracy (Acc.), (ii) sensitivity (Sen), and (iii) specificity (Spe), respectively defined as: (i) the second-by-second agreement between the two methods, (ii) the probability that behaviorally coded states were correctly identified by the algorithm, and (iii) the probability that epochs not behaviorally coded as a given state were correctly not labeled as that state by the algorithm. These three parameters were calculated with or without the transition points (inside and outside parenthesis, respectively). (Gervasoni, D. and Lin, S.C. et al. (2004). Global forebrain dynamics predict rat behavioral states and their transitions. *J Neurosci* 24(49): 11137–47.)

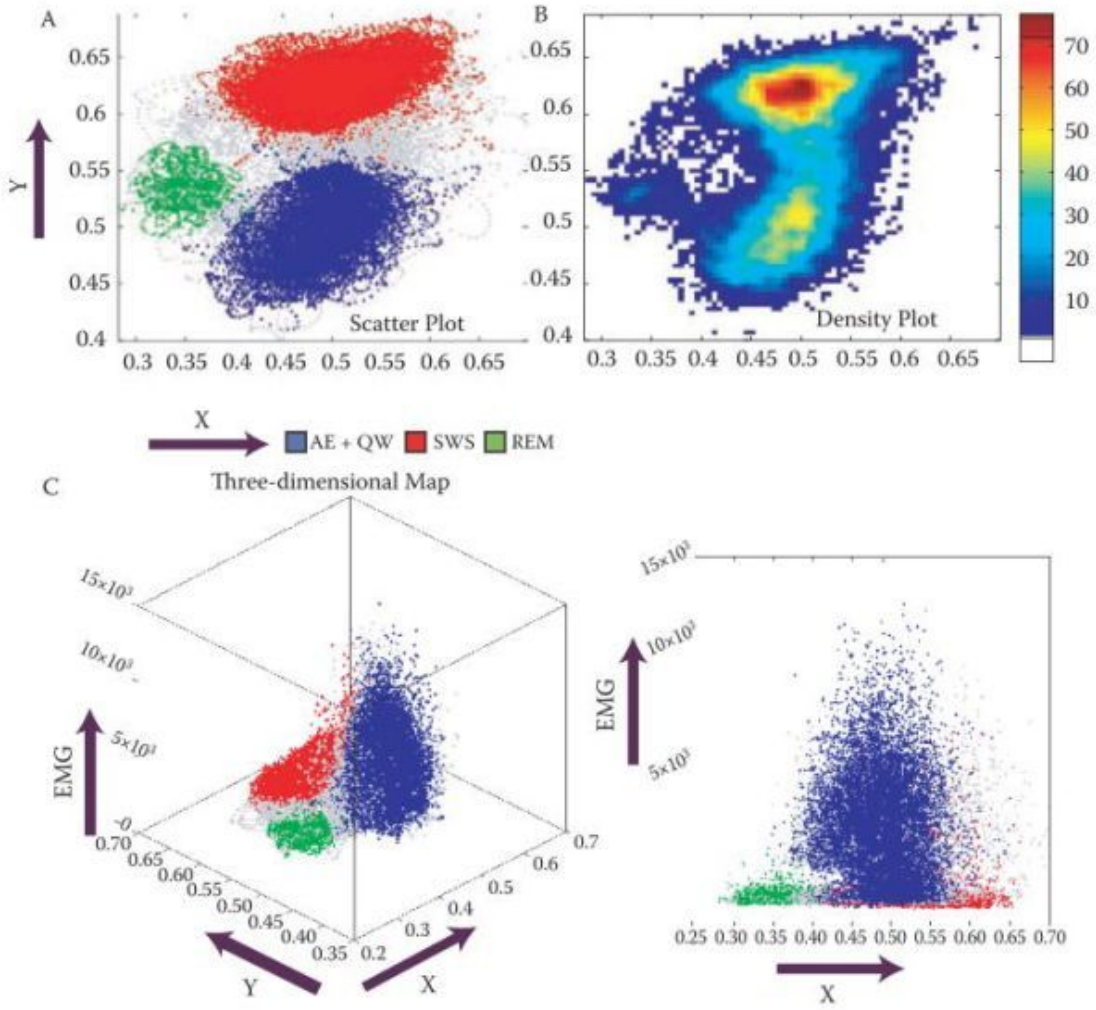

FIGURE 8.5

(See color insert following page 140.) Global brain states in mice. Scatter plot (A) and density plot (B) of the 2-D state space generated using hippocampal LFPs recorded in one mouse. Similar cluster structures as those described in rats (Figure 8.3A) were found. (C) Neck EMG amplitude was plotted as the third dimension (arbitrary unit), showing that the REM cluster had low or absent EMG activity, whereas the adjacent WK cluster showed maximal EMG activity. Two views represent two different projections of the same 3-D scatter plot.

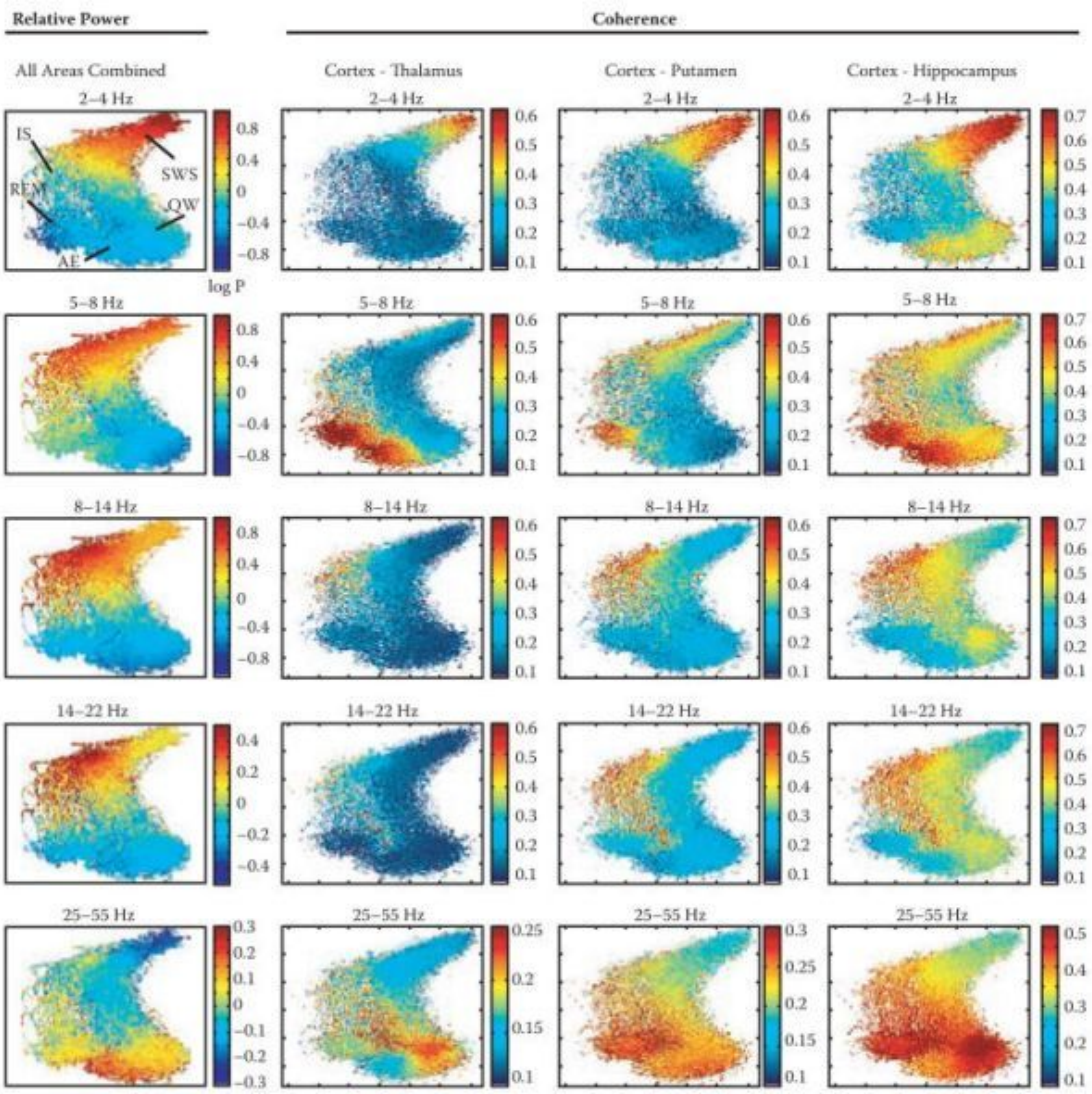

FIGURE 8.6

(See color insert following page 140.) Gradients within global brain states. Overlay of spectral power and coherence in different frequency bands on the 2-D state space of one rat. Spectral power was calculated on the log scale, averaged across all forebrain regions, with the mean log power subtracted. Thus, the amplitude represents the relative power above or below the mean value at each frequency band. Coherence was calculated for pairs of LFP channels as indicated. Several gradients were observed within global brain states: Note the high delta power and coherence during deep SWS (upper right end of the SWS cluster), while spindle power is higher at the other end of SWS cluster (shallow SWS). Also, within the WK cluster, active exploration (left end) and quiet awake (right end) showed prominent differences in the power and coherence at the theta and gamma frequency bands. In addition, the IS state was characterized by high power and coherence over a very broad frequency range. (Gervasoni, D. and Lin, S.C. et al. (2004). Global forebrain dynamics predict rat behavioral states and their transitions. *J Neurosci* 24(49): 11137–47.)

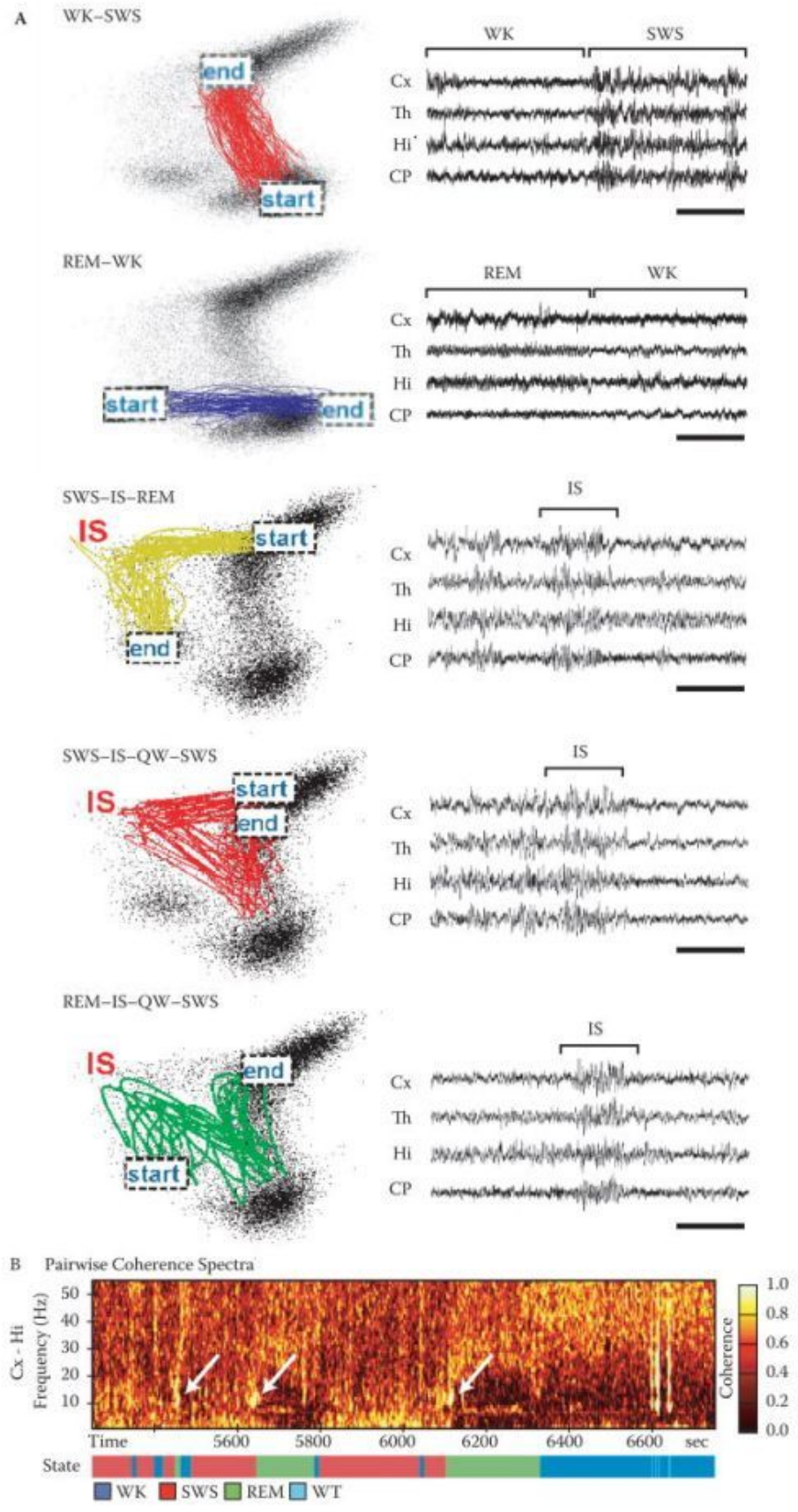

FIGURE 8.7

(see facing page) (See color insert following page 140.) Trajectory analysis. (A) Five state transition trajectories were illustrated, along with example LFP epochs. The first two trajectories, WK→SWS and REM→WK, represent typical fast state transitions with straight trajectories linking the two clusters. The other three trajectory

types all involve IS, including SWS→IS→REM, SWS→IS→WK and REM→IS→WK. Note that the IS state is accompanied by prominent oscillations present simultaneously in all forebrain regions (left panel). In the last two cases, trajectories directed toward SWS were shown, but the animal could remain in the WK state. (B) Pairwise coherence between Cx and Hi illustrating the state-dependent variations of coherence, aligned with behavioral states. The IS state (white arrows) shows high coherence in the 8–20 Hz range. (Gervasoni, D. and Lin, S.C. et al. (2004). Global forebrain dynamics predict rat behavioral states and their transitions. *J Neurosci* 24(49): 11137–47.)

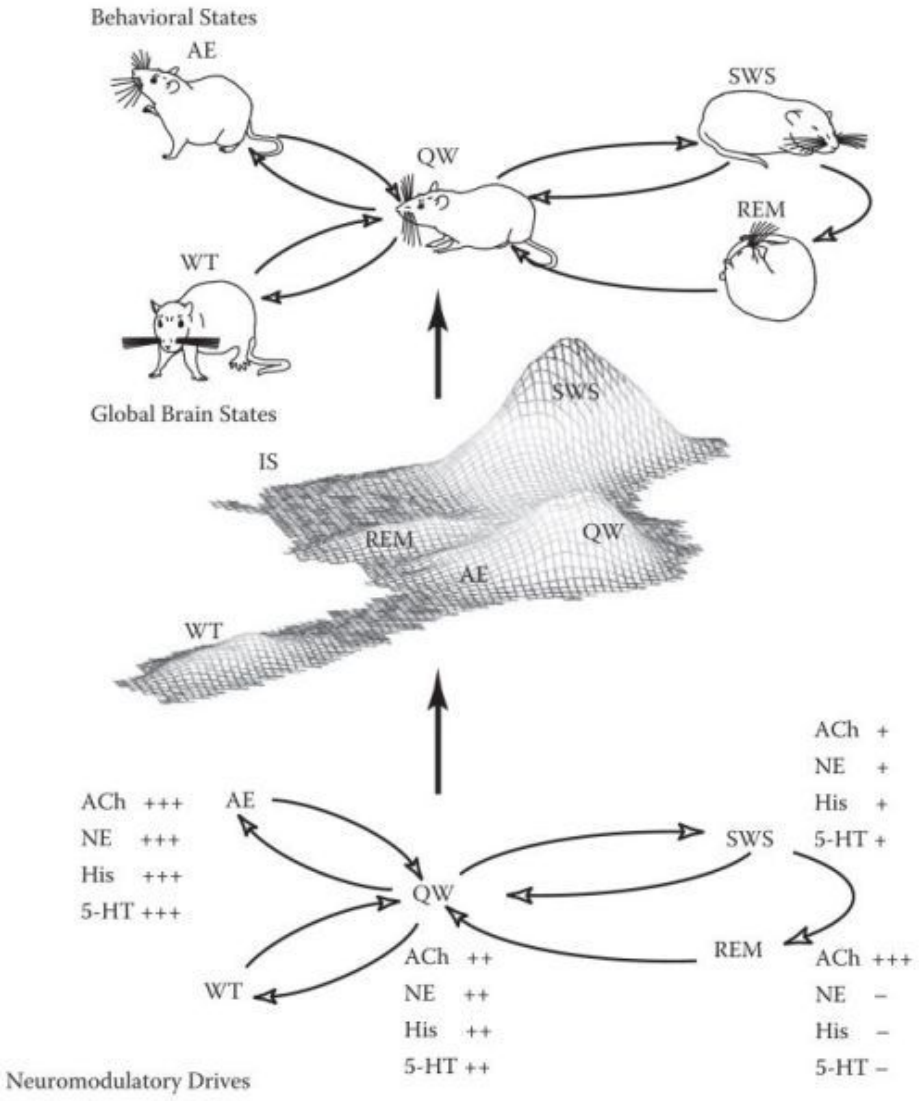

FIGURE 8.8

Global brain states reflect neuromodulatory drives and mediate behavioral states. The state space is represented in three dimensions (z-axis corresponds to the value in the density plot). The concerted influence of multiple neuromodulatory systems located in the basal forebrain, and the brainstem (bottom diagrams) shapes the dynamics in the forebrain network, resulting in global brain states. Global brain states, in turn, determine the state-specific modes of neuronal sensory processing and storage (see text).

Bookshelf ID: NBK3904 PMID: 21204450